J. Am. Soc. Mass Spectrom. (2011) 22:2171–2178
DOI: 10.1007/s13361-011-0243-4

RESEARCH ARTICLE

Blackbody Infrared Radiative Dissociation of Protonated Oligosaccharides

Messele A. Fentabil, Rambod Daneshfar, Elena N. Kitova, John S. Klassen

Alberta Innovates Centre for Carbohydrate Science and Department of Chemistry, University of Alberta, Edmonton, Alberta, CanadaT6G 2G2

Abstract

The dissociation pathways, kinetics, and energetics of protonated oligosaccharides in the gas phase were investigated using blackbody infrared radiative dissociation (BIRD). Time-resolved BIRD measurements were performed on singly protonated ions of cellohexaose (Cel_6), which is composed of β-(1→4)-linked glucopyranose rings, and five malto-oligosaccharides (Mal_x, where x=4–8), which are composed of α-(1→4)-linked glucopyranose units. At the temperatures investigated (85–160 °C), the oligosaccharides dissociate at the glycosidic linkages or by the loss of a water molecule to produce B- or Y-type ions. The Y ions dissociate to smaller Y or B ions, while the B ions yield exclusively smaller B ions. The sequential loss of water molecules from the smallest B ions (B_1 and B_2) also occurs. Rate constants for dissociation of the protonated oligosaccharides and the corresponding Arrhenius activation parameters (E_a and A) were determined. The E_a and A-factors measured for protonated Mal_x (x>4) are indistinguishable within error (~19 kcal mol^{-1}, 10^{10} s^{-1}), which is consistent with the ions being in the rapid energy exchange limit. In contrast, the Arrhenius parameters for protonated Cel_6 (24 kcal mol^{-1}, 10^{12} s^{-1}) are significantly larger. These results indicate that both the energy and entropy changes associated with the glycosidic bond cleavage are sensitive to the anomeric configuration. Based on the results of this study, it is proposed that formation of B and Y ions occurs through a common dissociation mechanism, with the position of the proton establishing whether a B or Y ion is formed upon glycosidic bond cleavage.

Key words: Oligosaccharides, Fragmentation, Blackbody infrared radiative dissociation, Kinetics, Energetics

Introduction

Carbohydrates, which are the most abundant biopolymer in nature, have many important functions. For example, biosynthesized polysaccharides serve as structural materials and energy sources [1]. Most membrane proteins and many extracellular proteins are glycosylated, as are many lipids. Glycolipids and glycoproteins are common cell surface components and are implicated in many important biological processes, including cell–cell communication, the immune response, and viral and bacterial infections [2]. The structures of oligosaccharides, either alone or as part of their glyconjugates, directly influence their function. Therefore, a comprehensive understanding of their functional roles requires detailed knowledge of their structures.

Mass spectrometry (MS) represents an important tool for the structural analysis of oligosaccharides. Positively charged (e.g., protonated or metal ion adducts) and negatively charged (e.g., deprotonated) oligosaccharide ions are readily produced in the gas phase using ionization techniques such as electrospray ionization (ES) and matrix assisted laser desorption ionization. Accurate mass measurements

Electronic supplementary material The online version of this article (doi:10.1007/s13361-011-0243-4) contains supplementary material, which is available to authorized users.

Correspondence to: John S. Klassen; *e-mail:* john.klassen@ualberta.ca

Received: 5 April 2011
Revised: 27 August 2011
Accepted: 30 August 2011
Published online: 22 September 2011

allow for the unambiguous assignment of the elemental composition of oligosaccharides. The gas phase ions may also be activated in order to induce their fragmentation (i.e., tandem MS, MS/MS or MS^n) [3–23]. From an analysis of the resulting fragment ions the sequence of sugar residues and their linkages and stereochemistry can also be determined. Analysis of the gas phase ions using ion mobility MS has also proven effective for differentiating isomeric carbohydrate structures [24–26].

A wide variety of activation techniques have been used to fragment oligosaccharide ions in the gas phase, although low energy collision-induced dissociation (CID) and infrared multiphoton dissociation (IRMPD) have been used most extensively [3–23]. Low energy CID and IRMPD of oligosaccharide ions generally results in cleavage of the glycosidic bonds [5, 6]. For singly charged, protonated and alkali-metal cationized oligosaccharides, cleavage of a glycosidic bond at the non-reducing side yields an oxacarbenium ion (referred to as a B-type ion) and a smaller neutral oligosaccharide [5]. Glycosidic bond cleavage may also be accompanied by proton transfer resulting in the formation of a smaller charged oligosaccharide (referred to as a Y-type ion) and a neutral epoxide [3, 5–7]. There is experimental evidence that it is an exchangeable hydrogen (e.g. from a neighboring hydroxyl group) that is transferred to produce Y ions [7]. The fragmentation mechanisms for protonated oligosaccharides are believed to be charge induced, whereby protonation of the glycosidic oxygen results in delocalization of the ring oxygen electrons and a concomitant weakening of the glycosidic bond [8]. Dissociation of alkali metal cationized oligosaccharides also leads to abundant B- and Y-type ions, in addition to fragments produced from cross ring cleavage reactions. For metal cationized oligosaccharides the metal ion coordinates with several oxygen atoms simultaneously such that there is little or no destabilization of the glycosidic bond. As a result higher energies are typically required to fragment metal cationized oligosaccharides, compared with protonated oligosaccharides [5, 9].

Despite the widespread application of tandem MS to characterize the structures of oligosaccharides, there have been relatively few studies of the dissociation mechanisms [7–19]. Perhaps the most detailed investigation into oligosaccharide fragmentation mechanisms is the recent study by Suzuki et al. [9]. These authors performed extensive calculations on a series of sodiated disaccharides of varying composition, linkage, and configuration, to estimate the dissociation activation energies and establish rules for fragmentation. However, to our knowledge, no quantitative experimental studies of the kinetics and energetics of oligosaccharide fragmentation reactions have been reported.

Here, we describe the first systematic study of the thermal dissociation of protonated oligosaccharide ions in the gas phase—their fragmentation pathways, kinetics, and energetics. Singly charged, protonated ions of a series of maltooligosaccharides (Mal_x, where x=4–8), which are composed of α-(1→4)-linked glucopyranose rings, and cellohexaose (Cel_6), which is composed of β-(1→4)-linked glucopyranose rings, were investigated using the blackbody infrared radiative dissociation (BIRD) technique [27, 28] and Fourier-transform ion cyclotron resonance (FTICR) MS. The BIRD mass spectra, together with the results of double resonance experiments, provide insights into the contribution of primary and secondary fragmentation pathways to the product ion mass spectra. More importantly, rate constants and Arrhenius parameters for the cleavage of glycosidic linkages were determined from time-resolved BIRD measurements. These data reveal that the anomeric configuration can have a dramatic effect on the kinetics and energetics of B and Y ion formation. Furthermore, the results of this study provide new insights into the mechanism of glycosidic bond cleavage in the gas phase.

Materials and Methods

Oligosaccharides

Maltotetraose (Mal_4), maltopentaose (Mal_5), maltohexaose (Mal_6), and maltoheptaose (Mal_7) were purchased from Sigma-Aldrich Canada (Oakville, Canada). Malto-octaose (Mal_8) and cellohexaose (Cel_6) were purchased from CarboSynth (Berkshire, UK). All of the oligosaccharides were used without further purification. ES was performed on aqueous solutions of each oligosaccharide (50 μM) and 2.5 mM ammonium acetate (pH 7) to produce singly protonated oligosaccharide ions in the gas phase.

Mass Spectrometry

All experiments were performed using a 9.4 T Bruker ApexII Fourier transform ion cyclotron resonance (FTICR) mass spectrometer (Billerica, MA) equipped with a nanoflow ES (nanoES) ion source. A detailed description of the instrument and the experimental conditions used for the BIRD measurements and the double resonance experiments can be found elsewhere [29].

Calculations

Geometry optimization calculations were performed on protonated Mal_4 using the AM1 semiempirical method implemented with Hyperchem 8.0 (Hypercube Inc., Gainesville, FL). The starting structure was obtained using the "Model Build" function and the proton was placed on the last glycosidic linkage at the reducing end. Vibrational frequencies were calculated for the energy-minimized structure.

Results and Discussion

BIRD of Protonated Oligosaccharides

The most abundant ions detected by ES-MS performed on aqueous solutions of 50 μM oligosaccharide in 2.5 mM ammonium acetate correspond to the singly protonated

oligosaccharide, together with the NH_4^+, Na^+ ,and K^+ adducts (Figure S1, Supplementary Data). Signal corresponding to protonated oligosaccharide ions minus one water molecule was also detected for all of the oligosaccharides investigated. These dehydrated ions are presumably formed in the ion source as a result of collisional heating of protonated oligosaccharide ions [30]. BIRD of the protonated Mal_x and Cel_6 ions was performed at temperatures ranging from 85 to 160 °C and reaction times ranging from 0.5 to 60 s. Shown in Figure 1a, b, and c are representative BIRD mass spectra acquired for $(Mal_6+H)^+$ at 100 °C and reaction times of 12, 26, and 60 s, respectively. At this and the other temperatures investigated, BIRD results predominantly in the formation of B- and Y-type ions; a complete series of B ions was observed (B_1–B_6) and a partial Y ion series (Y_4 and Y_5 ions). The sequential dehydration of the B_1 and B_2 ions, resulting in (B_1–H_2O), (B_1–$2H_2O$), (B_2–$2H_2O$), and (B_2–$3H_2O$) ions, also occurs and these ions dominate at longer reaction times. BIRD of the other protonated Mal_x ions resulted in the formation of similar products ions, i.e., B_1–B_x, Y_4–Y_{x-1}, (B_1–H_2O), (B_1–$2H_2O$), (B_2–$2H_2O$), and (B_2–$3H_2O$) ions. The fragmentation of protonated Cel_6 yielded similar product ions although higher reaction temperatures were required to achieve extensive fragmentation (Figure 2a and b).

The Y ions observed in the BIRD mass spectra result from the cleavage of the glycosidic bonds, on non-reducing side, either directly from the reactant ion (i.e., via one of several parallel pathways) or from secondary fragmentation of Y ions, which are themselves protonated oligosaccharides. The B ions can also be produced by multiple reaction pathways. For a given reactant ion (e.g., protonated Mal_x),

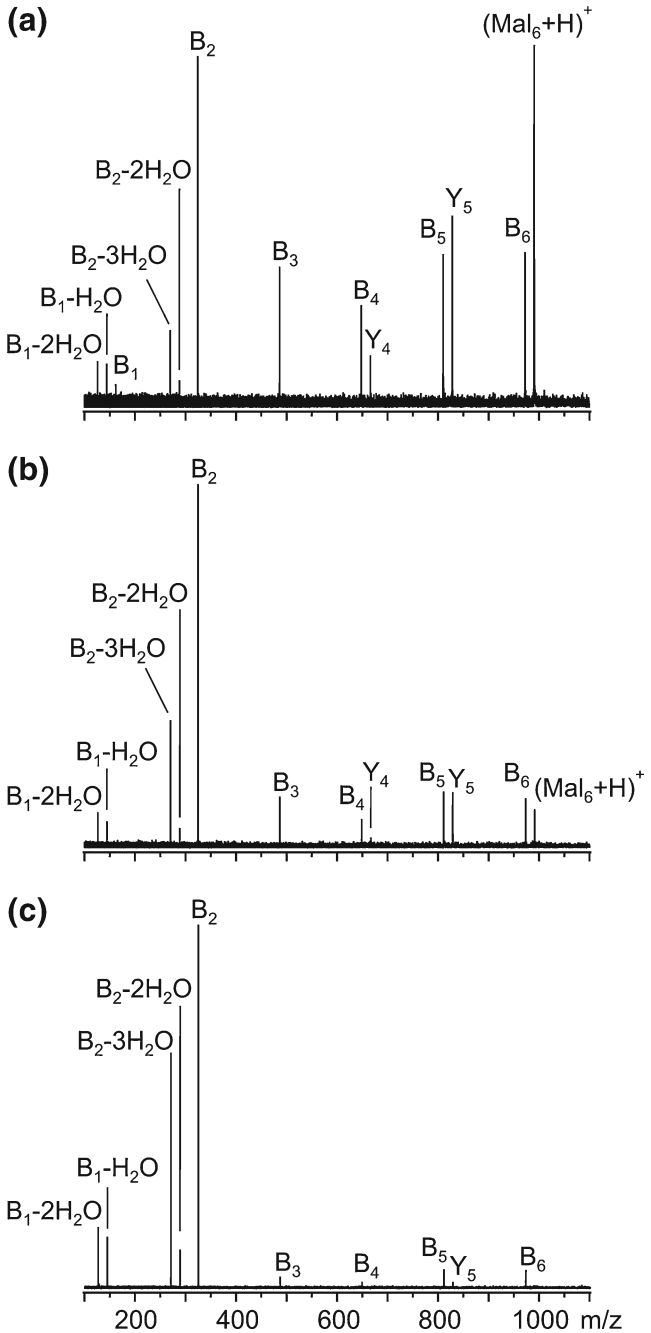

Figure 1. BIRD mass spectra acquired for $(Mal_6+H)^+$ at a reaction temperature of 100 °C and reaction times of (**a**) 12 s, (**b**) 26 s, and (**c**) 60 s

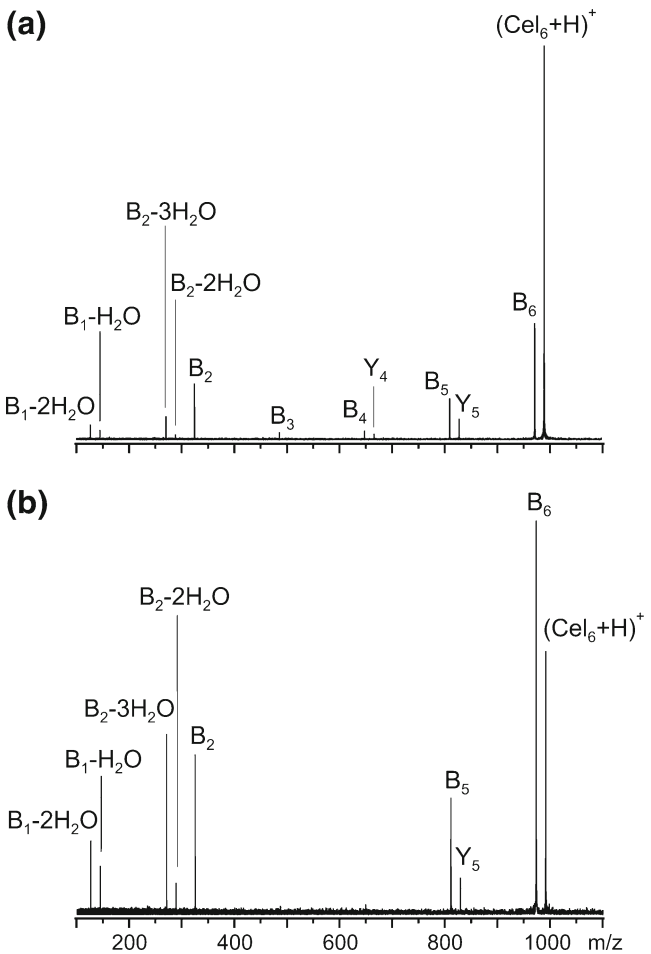

Figure 2. BIRD mass spectra acquired for $(Cel_6+H)^+$ at a reaction temperature of 118 °C and reaction times of (**a**) 15 s and (**b**) 60 s

the corresponding B_x ion is produced by the loss of H_2O. Smaller B ions can also be produced from primary fragmentation (through glycosidic bond cleavage) or from Y product ions (by glycosidic bond cleavage or water loss). Cleavage of the glycosidic bonds of the B ions can also lead to smaller B ions, vide infra. Sequential water loss has been observed in CID experiments performed on protonated (or ammonium adducts) ions of some monosaccharides [7] and oligosaccharides [8]. For example, CID of the ammonium adducts of xylopentaose leads to B ions that have lost up to five water molecules [8]. The proposed mechanism for water loss from B ions involves the formation of aromatic ring structures at the reducing end of the oligosaccharide. Interestingly, sequential water loss was not observed in CID of ammonium adducts of Mal_5 and it was suggested that the process is blocked by the CH_2OH group at the C-5 position. However, the present results clearly indicate that water loss can occur, at least from the smaller B ions.

BIRD of B Ions

BIRD measurements were also performed on B_2–B_6 ions. The B_2, B_3, and B_4 reactant ions were produced by BIRD of protonated Mal_4, while the B_5 and B_6 ions were produced from protonated Mal_6. Shown in Figure 3 are representative BIRD mass spectra measured for the B_6 ion at 109 °C and reaction times of 1 and 8 s. Signals corresponding to B_2–B_5 ions, along with the (B_2–$3H_2O$) ion, were detected. At longer times, B_1, (B_1–H_2O), (B_1–$2H_2O$), and (B_2–$2H_2O$) ions were also detected (data not shown). Similar results were obtained for the other B_x ions investigated. It is interesting to note that the timescales for the dissociation of the B_x ions are comparable to those of the protonated Mal_x ions, despite the absence of an excess proton to induce cleavage of the glycosidic bonds. The significance of this observation is discussed below.

Double Resonance Experiments

In an effort to further probe the contribution of different dissociation pathways to the BIRD mass spectra, double resonance experiments were performed on the fragment ions produced from the $(Mal_6+H)^+$ ion. For these measurements, BIRD mass spectra were acquired at a reaction temperature of 117 °C and a 6.5 s reaction time with the application of continuous rf excitation at the cyclotron frequency corresponding to a particular product ion. The rf excitation causes the selected product ion to be ejected from the ion cell, as it is formed, thereby eliminating the possibility of secondary fragmentation. A decrease in the relative abundance of smaller product ions serves to identify ions originating either directly or indirectly from that particular product ion. Listed in Table 1 are the ratios of the intensity of individual product ions over that of the reactant ion measured following the continuous ejection of a particular product ion. Based on these results, it is possible to conclude that secondary

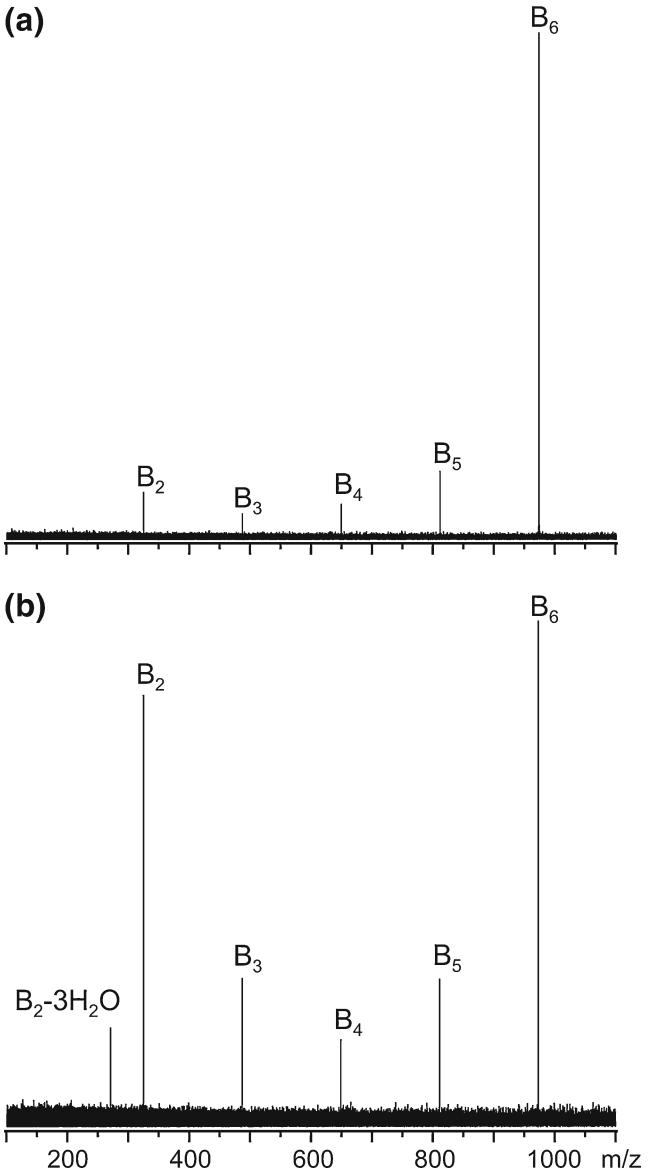

Figure 3. BIRD mass spectra acquired for B_6 ion, which was produced from protonated Mal_6, at a reaction temperature of 109 °C and reaction times of (**a**) 1 s and (**b**) 8 s

fragmentation of the B_x ions leads both directly or indirectly (through sequential fragmentation reactions) to each of the smaller B_x ions. It is also interesting to note that ejection of B_2 results in a nearly complete loss of not only the (B_2–$2H_2O$) and (B_2–$3H_2O$) ions but also the B_1, (B_1–H_2O) and (B_1–$2H_2O$) ions. These results indicate that B_2 represents the major precursor of the B_1 ion and dehydrated B_1 and B_2 ions.

Dissociation Kinetics and Arrhenius Parameters

The temperature-dependent dissociation rate constants (k) were determined from changes in the natural log of the normalized intensity of the protonated oligosaccharide ions

Table 1. Summary of BIRD double resonance experiments obtained for the $(Mal_6+H)^+$ ion at 117 °C and 6.5 s. Listed are the ratios of the intensity of individual product ions to the reactant ion measured while ejecting one of the product ions (indicated by **X**) by applying continuous rf excitation at the corresponding cyclotron frequency

B_1**	B_1*	B_1	B_2***	B_2**	B_2	B_3	B_4	Y_4	B_5	Y_5	B_6	Mal_6
0.2	0.2	0.1	0.4	0.1	2.1	1.1	0.6	0.3	0.8	0.8	0.7	1
0.2	0.2	0.1	0.3	0.1	1.3	0.6	0.3	0.3	0.3	0.8	**X**	1
0.2	0.2	0.1	0.3	0.1	1.6	0.8	0.5	0.1	0.7	**X**	0.7	1
0.2	0.2	0.1	0.3	0.1	1.0	0.4	0.2	0.3	**X**	0.8	0.7	1
0.2	0.2	0.1	0.4	0.1	1.5	0.8	0.5	**X**	0.8	0.8	0.7	1
0.2	0.1	0.1	0.2	0.0	0.5	0.2	**X**	0.3	0.8	0.8	0.7	1
0.1	0.1	0.0	0.1	0.0	0.2	**X**	0.6	0.3	0.8	0.8	0.7	1
0.1	0.0	0.0	0.0	0.0	**X**	1.1	0.7	0.3	0.8	0.8	0.7	1

The first row corresponds to ion intensity ratios measured by BIRD at 117 °C and 6.5 s reaction time. The asterisk(s) (*), (**), and (***) represents the loss of one, two, and three water molecules, respectively, from the B_1 and B_2 ions.

($I_{R,norm}$) with reaction time (Equation 1):

$$\ln\left(I_{R,norm}\right) = -kt \quad (1)$$

The $I_{R,norm}$ term was calculated using Equation 2, where I_R is the intensity of the reactant ion and ΣI_P is the sum of the intensities of all product ions, including those produced by secondary reactions:

$$I_{R,norm} = I_R/(I_R + \Sigma I_P) \quad (2)$$

Illustrative kinetic plots obtained for $(Mal_6+H)^+$ and $(Cel_6+H)^+$ ion, at five different temperatures, are shown in Figure 4. The plots are linear and, in most cases, exhibit near zero intercepts. Plots of similar quality were obtained for the other reactant ions investigated. The value of k was determined from the slope of a linear least squares fit of the kinetic data measured at each temperature investigated.

That the kinetic plots are linear can be interpreted in several ways. Linear plots are expected when the reactant exists in a single dominant structure or multiple, rapidly interconverting structures. Alternatively, and perhaps less likely, linear plots will arise when the reactant exists in multiple, non-interconverting structures, each of which reacts with the same or very similar kinetic parameters. Given that primary fragmentation of the protonated oligosaccharide ions occurs at multiple glycosidic bonds it is possible that each oligosaccharide ion exists in multiple, rapidly interconverting structures. These rapid structural fluctuations may be accompanied by proton transfer between carbohydrate residues, similar to the mobile proton model proposed for the fragmentation of protonated peptides in the gas phase [31].

Time-resolved BIRD measurements were also performed on the B_x ions, where x=2–6, produced by water loss from the corresponding protonated Mal_x ions. Shown in Figure S2 are the illustrative kinetic data measured at ~100 °C. Notably, the kinetic plots are, in all cases, non-linear. As a result, it was not possible to extract reliable dissociation rate constants. These results indicate that the B_x ions exist in multiple, kinetically distinct structures. At present, however, it is not known whether the multiple structures reflect

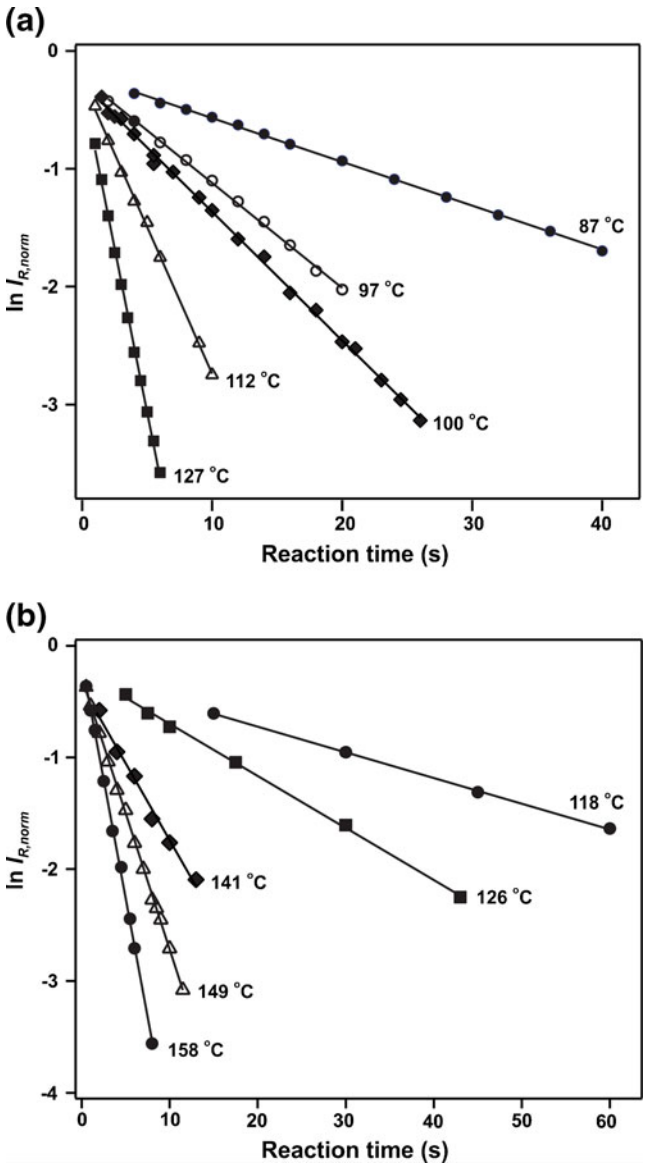

Figure 4. Plots of the natural logarithm of the normalized intensity, ln ($I_{R,norm}$), of (**a**) $(Mal_6+H)^+$ and (**b**) $(Cel_6+H)^+$ versus reaction time measured at the temperatures indicated

differences in the location of the charge or whether a given B ion can adopt multiple conformations.

Arrhenius plots, constructed from the temperature-dependent *k* values measured for dissociation of protonated Mal_x and Cel_6 ions, are shown in Figure 5. The Arrhenius activation energy (E_a) and pre-exponential factor (A) were obtained from the slope and y-intercept, respectively, of a linear least squares fit of the kinetic data and the values are listed in Table 2. Also listed are the entropies of activation ($\Delta S^{\ddagger}$), the difference in entropy between the transition state and the reactant, which were calculated at 120 °C (the median reaction temperature) from the corresponding A-factor using Equation 3:

$$A = (ek_BT/h)\exp\left(\Delta S^{\ddagger}/R_g\right) \quad (3)$$

where k_B, h, and R_g are the Boltzmann constant, Planck constant, and gas constant, respectively.

Inspection of the Arrhenius plots and the corresponding parameters listed in Table 2 reveals a number of interesting features. The E_a and A values determined for the protonated Mal_x ions, with x=5–8, are indistinguishable, within experimental error (19 kcal mol^{-1} and 10^{10} s^{-1}). In contrast, the Arrhenius parameters determined for protonated Mal_4 are significantly smaller (14 kcal mol^{-1} and 10^8 s^{-1}), while those for protonated Cel_6 are larger (24 kcal mol^{-1} and 10^{12} s^{-1}). The similarity in the parameters measured for the larger Mal_x ions suggests that these ions are in or are close to being in the rapid energy exchange (REX) limit, such that their internal energy is described by a Boltzmann distribution [32]. Given the relatively small size of these ions, with masses ranging from 667 (Mal_4) to 1315 Da (Mal_8), this result is, perhaps, surprising. Williams and coworkers have modeled the dissociation kinetics of a protonated peptide polymer, $(Ala\text{-}Gly)_n$, activated by blackbody radiation as a function of size and Arrhenius parameters [32]. For dissociation reactions with Arrhenius parameters of similar

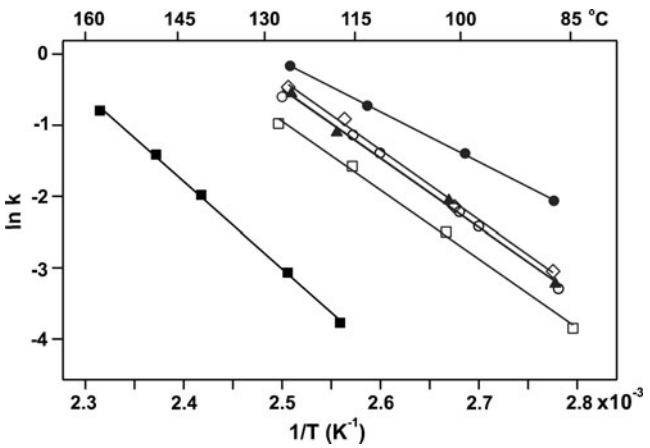

Figure 5. Arrhenius plots for the dissociation of the $(Cel_6+H)^+$ (filled square) and $(Mal_x+H)^+$ ions, where x=4 (filled circle), 5 (open square), 6 (open circle), 7 (filled triangle) and 8 (open diamond)

Table 2. Arrhenius activation parameters (E_a, A) and the corresponding entropies of activation ($\Delta S^{\ddagger}$) measured for the dissociation of singly protonated Mal_x, where x=4–8, and Cel_6 ions

Oligosaccharide	E_a (kcal mol^{-1})[a]	A (s^{-1})[a]	$\Delta S^{\ddagger}$ (cal K^{-1} mol^{-1})[b]
Mal_4	14.0±0.2	$10^{7.6\pm0.1}$	−26.3±0.5
Mal_5	19.2±0.7	$10^{10.1\pm0.4}$	−14.9±1.8
Mal_6	19.3±0.7	$10^{10.3\pm0.4}$	−13.9±1.9
Mal_7	19.3±0.8	$10^{10.3\pm0.5}$	−13.9±2.3
Mal_8	19.5±0.7	$10^{10.4\pm0.4}$	−13.5±1.8
Cel_6	24.3±0.4	$10^{12.0\pm0.2}$	−6.2±0.9

[a] Errors correspond to one standard deviation.
[b] Values calculated at 393 K.

magnitude to those measured for the larger Mal_x ions, i.e., 18 kcal mol^{-1} and 10^{10} s^{-1}, their analysis revealed that the REX limit is achieved at molecular weights of ~3 kDa. However, according to their analysis, for peptide ions with molecular weights comparable to those of the Mal_x ions investigated here, the difference between the apparent and true energy barrier is expected to be less than 5% [32]. It should also be pointed out that the IR spectra of the oligosaccharides investigated here are expected to be quite different from that of protonated $(Ala\text{-}Gly)_2$. Shown in Figure S3 is the IR spectrum calculated at the AM1 level of theory for a minimized structure of protonated Mal_4. Notably, there is significantly greater overlap of the oligosaccharide vibrational frequencies and the Planck radiation distributions at the BIRD reaction temperatures than found for $(Ala\text{-}Gly)_2$ [32]. It follows that for reactions proceeding with similar kinetic parameters, the minimum molecular weight required to achieve the REX limit will be smaller for oligosaccharides than for peptides. Based on these considerations, it is reasonable to conclude that the E_a values measured for the dissociation of protonated Cel_6 and Mal_x (where x>4) ions in the present study are within 1 kcal mol^{-1} of the true E_a values.

It follows then that the average E_a values for the cleavage of glycosidic bonds in α-(1→4)-linked and β-(1→4)-linked glucopyranose rings are approximately 19 and 24 kcal mol^{-1}, respectively. That the fragmentation of the protonated Mal_6 ion occurs with lower E_a than protonated Cel_6 is consistent with earlier observations that α glycosidic bonds cleave more easily than β glycosidic bonds in CID experiments [8]. As discussed by Suzuki *et al.* [9], the lower stability of the α glycosidic bonds can be explained in terms of the anomeric effect. Hyperconjugation between one of the lone electron pairs of the ring oxygen and the σ* orbital of the C–O bond is possible for α glycosides, but not for β glycosides. Because of this electron delocalization, the energy barrier for C1–O bond cleavage in the α glycosides is expected to be lower than for the β glycosides [9].

While there are no comparable experimental data for the energy barrier to glycosidic bond cleavage reactions for metal cationized oligosaccharide ions, it is interesting to compare the E_a values measured for protonated Mal_x and Cel_6 ions with those calculated [using the HF/6-31 G(d)

basis set] for cleavage of the glycosidic bond in the $(Mal_2+Na)^+$ and $(Cel_2+Na)^+$ [9]. According to these calculations, the energy barriers for the formation of B/Y ions from Mal_2 and Cel_2 are ~60 and ~100 kcal mol^{-1}, respectively. These values are significantly larger than the E_a values determined in the present study. Assuming that the calculated values accurately reflect the true dissociation E_a values, these results highlight the significant effect that the charging agent can have on the stability of the glycosidic bonds in the gas phase.

It is also important to comment on the A-factors determined for the dissociation of the protonated Mal_x and Cel_6 ions. The measured values, which range from 10^8 to 10^{12} s^{-1}, correspond to negative $\Delta S^{\ddagger}$ values (−26 to −6 cal mol^{-1} K^{-1} at 120 °C) and suggest that the reactions leading to cleavage of the glycosidic bonds proceed through relatively tight transition states (TS), in which there is a loss of conformational flexibility. In the case of Y ion formation, which requires that a hydrogen atom be transferred from a neighboring hydroxyl group to the glycosidic oxygen at the site of cleavage, a constrained TS is to be expected. However, it is more difficult to rationalize a tight TS for B ion formation. Assuming the rate limiting step for B ion formation involves cleavage of the glycosidic linkage following protonation of the oxygen atom [7], a loose TS (with a positive $\Delta S^{\ddagger}$) is expected. The small A-factors established from the BIRD measurements would seem to suggest that this view of B ion formation is incorrect or, at the very least, that the rate limiting step does not involve simple bond fission. This finding, taken together with the observation that glycosidic linkages of B ions dissociate with similar kinetics as those measured for the protonated oligosaccharides, raises the possibility that protonation of the glycosidic oxygen does not precede bond cleavage [10]. Instead, it is possible that the formation of B and Y ions occurs through a common dissociation mechanism involving hydrogen transfer from a neighboring hydroxyl group to the glycosidic oxygen, with the position of the excess proton establishing whether a B or Y ion is formed (Scheme 1). This putative mechanism is similar to the mechanism proposed for B and Y ion formation from metal cationized oligosaccharides [9]. A computational study has been initiated by our laboratory to further investigate the mechanism(s) of glycosidic bond fragmentation in these and other protonated oligosaccharides.

Conclusions

The present study represents the first investigation into the thermal dissociation of protonated oligosaccharides in the gas phase. Time-resolved BIRD measurements were performed on singly protonated Cel_6, which is composed of β-(1→4)-linked glucopyranose rings, and protonated Mal_x (where x=4–8) ions, which are composed of α-(1→4)-linked glucopyranose rings. Over the range of temperatures investigated, the oligosaccharides were found to undergo cleavage of the glycosidic linkages and the loss of water, as parallel processes, to give B- or Y-type ions. The primary B and Y fragment ions readily undergo secondary fragmentation; the Y ions dissociate to smaller Y ions as well as to B ions, while the B ions yield smaller B ions. Sequential water loss from the smallest B ions (B_1 and B_2) also readily occurs. Apparent rate constants for the dissociation of the protonated oligosaccharides, reflecting the multiple primary

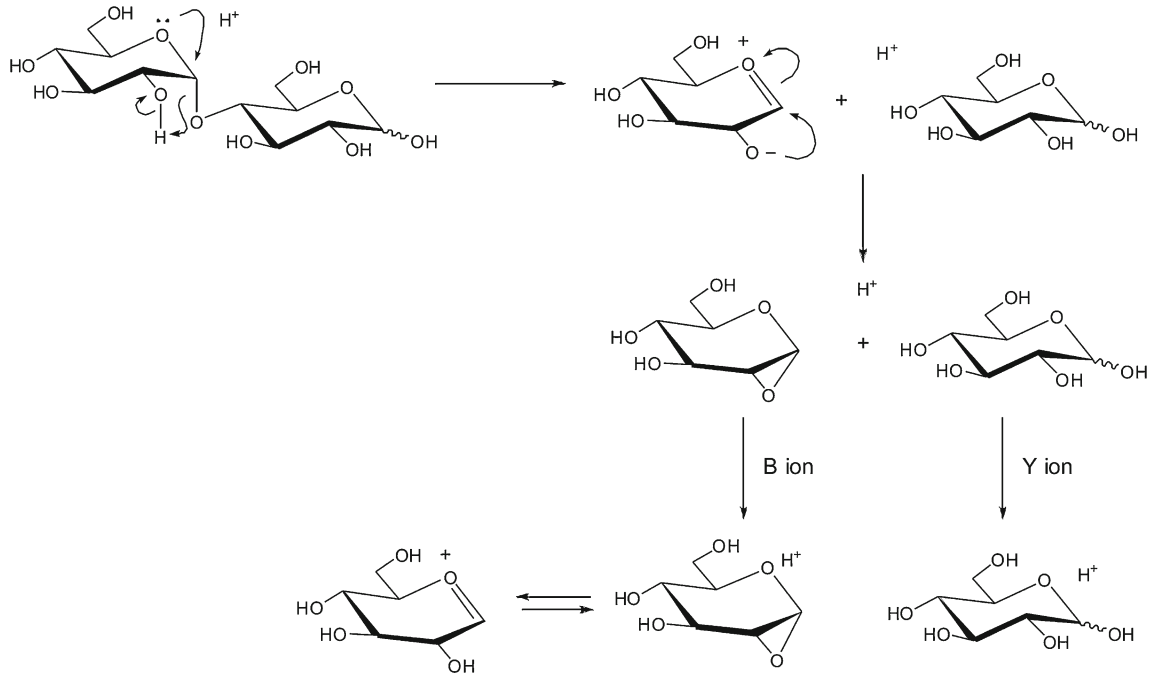

Scheme 1. Proposed reaction mechanism of fragmentation of glycosyl bond in protonated maltodisaccharide

dissociation channels, were measured and the corresponding Arrhenius parameters were determined. The E_a and A-factors measured for protonated Mal_x (where $x>4$) are indistinguishable within error. This finding suggests that the REX limit is achieved by the protonated oligosaccharide ions in the BIRD experiments. Notably, the Arrhenius parameters measured for protonated Cel_6 are significantly larger than for protonated Mal_6; these results demonstrate that both the energy and entropy changes associated with the cleavage of glycosidic bonds are sensitive to the anomeric configuration. Finally, the results of this study raise the possibility that protonation of the glycosidic oxygen does not precede bond cleavage. Instead, it is proposed that the formation of B and Y ions may occur through a common dissociation mechanism, with the position of the proton establishing whether a B or a Y ion is formed upon glycosidic bond cleavage.

Acknowledgment

The authors acknowledge the Natural Sciences and Engineering Research Council of Canada and the Alberta Innovates Centre for Carbohydrate Science for generous funding and thank Professor T. Lowary (University of Alberta) for many helpful discussions.

References

1. Dwek, R.A.: Glycobiology: Toward Understanding the Function of Sugars. *Chem. Rev* **96**, 683–720 (1996)
2. Dwek, R.A., Butters, T.D.: Glycobiology—Understanding the Language and Meaning of Carbohydrates. *Chem. Rev* **102**, 283–284 (2002)
3. Domon, B., Costello, C.E.: A systematic nomenclature for carbohydrate fragmentations in FAB-MS/MS spectra of glycoconjugates. *Glycoconj. J* **5**, 397–409 (1988)
4. Reinhold, V.N., Reinhold, B.B., Costello, C.E.: Carbohydrate Molecular Weight Profiling, Sequence, Linkage, and Branching Data: ES-MS and CID. *Anal. Chem* **67**, 1772–1784 (1995)
5. Zaia, J.: Mass spectrometry of oligosaccharides. *Mass Spectrom. Rev* **23**, 161–227 (2004)
6. Electrospray and MALDI Mass Spectrometry: Fundamentals, Instrumentation, Practicalities, and Biological Applications, 2nd edn. In: Cole, R.B. (ed.). John Wiley and Sons (2010)
7. Yamagaki, T., Fukui, K., Tachibana, K.: Analysis of Glycosyl Bond Cleavage and Related Isotope Effects in Collision-Induced Dissociation Quadrupole-Time-of-Flight Mass Spectrometry of Isomeric Trehaloses. *Anal. Chem* **78**, 1015–1022 (2006)
8. Pasanen, S., Jänis, J., Vainiotalo, P.: Cello-, Malto-, and Xylo-Oligosaccharide Fragmentation by Collision-Induced Dissociation Using QIT and FT-ICR Mass Spectrometry: A Systematic Study. *Int. J. Mass Spectrom* **263**, 22–29 (2007)
9. Suzuki, H., Kameyama, A., Tachibana, K., Narimatsu, H., Fukui, K.: Computationally and Experimentally Derived General Rules for Fragmentation of Various Glycosyl Bonds in Sodium Adduct Oligosaccharides. *Anal. Chem* **81**, 1108–1120 (2009)
10. Ngoka, L.C., Gal, J.F., Lebrilla, C.B.: Effects of Cations and Charge Types on the Metastable Decay Rates of Oligosaccharides. *Anal. Chem* **66**, 692–698 (1994)
11. Kurimoto, A., Daikoku, S., Mutsuga, S., Kanie, O.: Analysis of Energy-Resolved Mass Spectra at MS^n in a Pursuit to Characterize Structural Isomers of Oligosaccharides *Anal. Chem* **78**, 3461–3466 (2006)
12. Cancilla, M.T., Penn, S.G., Carroll, J.A., Lebrilla, C.B.: Coordination of Alkali Metals to Oligosaccharides Dictates Fragmentation Behavior in Matrix Assisted Laser Desorption Ionization/Fourier Transform Mass Spectrometry. *J. Am. Chem. Soc* **118**, 6736–6745 (1996)
13. Berman, E.S.F., Kulp, K.S., Knize, M.G., Wu, L., Nelson, E.J., Nelson, D.O., Wu, K.J.: Distinguishing Monosaccharide Stereo- and Structural Isomers with TOF-SIMS and Multivariate Statistical Analysis. *Anal. Chem* **78**, 6497–6503 (2006)
14. Domon, B., Mueller, D.R., Richter, W.J.: Tandem Mass Spectrometric Analysis of Fixed-Charge Derivatized Oligosaccharides. *Org. Mass Spectrom* **29**, 713–719 (1994)
15. Bosso, C., Heyraud, A., Patron, L.: Oligosaccharide Characterizations by Fast Atom Bombardment Mass Spectrometry. Fragmentation Study in Relation to the Substituent at the Reducing End *Org. Mass Spectrom* **26**, 321–334 (1991)
16. Denekamp, G., Sandlers, Y.: Anomeric Distinction and Oxonium Ion Formation in Acetylated Glycosides. *J. Mass Spectrom* **40**, 765–771 (2005)
17. Fang, T.T., Zirrolli, J., Bendiak, B.: Differentiation of the Anomeric Configuration and Ring Form of Glucosyl-Glycolaldehyde Anions in the Gas Phase by Mass Spectrometry: Isomeric Discrimination Between *m/z* 221 Anions Derived from Disaccharides and Chemical Synthesis of *m/z* 221 Standards. *Carbohydr. Res* **342**, 217–235 (2007)
18. Fang, T.T., Bendiak, B.: The Stereochemical Dependence of Unimolecular Dissociation of Monosaccharide- Glycolaldehyde Anions in the Gas Phase: A Basis for Assignment of the Stereochemistry and Anomeric Configuration of Monosaccharides in Oligosaccharides by Mass Spectrometry via a Key Discriminatory Product Ion of Disaccharide Fragmentation, *m/z* 221. *J. Am. Chem. Soc* **129**, 9721–9736 (2007)
19. Bendiak, B., Fang, T.T.: Assignment of the Stereochemistry and Anomeric Configuration of Structurally Informative Product Ions Derived from disaccharides: Infrared Photodissociation of Glycosyl-Glycolaldehydes in the Negative Ion Mode. *Carbohydrate Res* **345**, 2390–2400 (2010)
20. Polfer, N.C., Valle, J.J., Moore, D.T., Oomens, J., Eyler, J.R., Bendiak, B.: Differentiation of Isomers by Wavelength-Tunable Infrared Multiple-Photon Dissociation-Mass Spectrometry: Application to Glucose-Containing Disaccharides. *Anal. Chem* **78**, 670–679 (2006)
21. Cagmat, E.B., Szczepanski, J., Pearson, W.L., Powell, D.H., Eyler, J.R., Polfer, N.C.: Vibrational Signatures of Metal-chelated Monosaccharide Epimers: Gas-phase Infrared Spectroscopy of Rb^+-tagged Glucuronic and Iduronic Acid. *Phys. Chem. Chem. Phys* **12**, 3474–3479 (2010)
22. Stefan, S.E., Eyler, J.R.: Differentiation of Methyl-glucopyranoside Anomers by Infrared Multiple Photon Dissociation with a Tunable CO_2 Laser; *Anal. Chem* **81**, 1224–1227 (2009)
23. Stefan, S.E., Eyler, J.R.: Differentiation of Glucose-Containing Disaccharides by Infrared Multiple Photon Dissociation with a Tunable CO_2 Laser and Fourier Transform Ion Cyclotron Resonance Mass Spectrometry. *Int. J. Mass Spectrom* **297**, 96–101 (2010)
24. Clowers, B.H., Dwivedi, P., Steiner, W.E., Hill, H.H. Jr., Bendiak, B.: Separation of Sodiated Isobaric Disaccharides and Trisaccharides Using Electrospray Ionization Atmospheric Pressure Ion Mobility Time of Flight Mass Spectrometry. *J. Am. Soc. Mass Spectrom* **16**, 660–669 (2005)
25. Dwivedi, P., Bendiak, B., Clowers, B.H., Hill, H.H. Jr.: Rapid Resolution of Carbohydrate Isomers by Electrospray Ionization Ambient Pressure Ion Mobility Spectrometry-Time-of-Flight Mass Spectrometry (ESI-APIMS-TOFMS). *J. Am. Soc. Mass Spectrom* **18**, 1163–1175 (2007)
26. Zhu, M., Bendiak, B., Clowers, B., Hill, H.H. Jr.: Ion Mobility-Mass Spectrometry Analysis of Isomeric Carbohydrate Precursor Ion. *Anal. Bioanal. Chem* **394**, 1853–1867 (2009)
27. Dunbar, R.C., McMahon, T.B.: Activation of Unimolecular Reactions by Ambient Blackbody Radiation. *Science* **279**, 194–197 (1998)
28. Price, W.D., Schnier, P.D., Jockusch, R.A., Strittmatter, E.R., Williams, E.R.: Unimolecular Reaction Kinetics in the High-Pressure Limit without Collisions. *J. Am. Chem. Soc* **118**, 10640–10644 (1996)
29. Daneshfar, R., Klassen, J.S.: Arrhenius Activation Parameters for the Loss of Neutral Nucleobases from Deprotonated Oligonucleotide Anions in the Gas Phase. *J. Am. Soc. Mass Spectrom* **15**, 55–64 (2004)
30. Wang, W., Kitova, E.N., Klassen, J.S.: Influence of Solution and Gas Phase Processes on Protein-Carbohydrate Binding Affinities Determined by Nanoelectrospray Fourier-Transform Ion Cyclotron Resonance Mass Spectrometry. *Anal. Chem* **75**, 4945–4955 (2003)
31. Wysocki, V.H., Tsaprailis, G., Smith, L.L., Breci, L.A.: Mobile and Localized Protons: A Framework for Understanding Peptide Dissociation. *J. Mass Spectrom* **35**, 1399–1406 (2000)
32. Price, W.D., Williams, E.R.: Activation of Peptide Ions by Blackbody Radiation: Factors That Lead to Dissociation Kinetics in the Rapid Energy Exchange Limit. *J. Phys. Chem. A* **101**, 8844–8852 (1997)